Materials Chemistry and Physics 257 (2021) 123821

Contents lists available at ScienceDirect

Materials Chemistry and Physics

journal homepage: www.elsevier.com/locate/matchemphys

Mechanical and thermal properties of modified Georgian and Brazilian clay infused biobased epoxy nanocomposites

Deepa Kodali [a], Md-Jamal Uddin [a], Esperidiana A.B. Moura [b], Vijay K. Rangari [a,*]

[a] Department of Materials Science and Engineering, Tuskegee University, Tuskegee, AL, 36088, USA
[b] Nuclear and Energy Research Institute, IPEN-CNEN/SP, Av. Prof. L. Prestes, 2242, Zip Code 05508-000, Sao Paulo, Brazil

HIGHLIGHTS

- Functionalized Georgian and Brazilian clay infused epoxy resin nanocomposites were developed.
- The synthesis was carried out using mechano-chemical attrition and ultrasound irradiation techniques.
- Addition of nanoclay particles improved thermal and mechanical properties.
- Georgian and Brazilian clay nanoparticles were proved to be effective fillers when used in moderate quantities.

GRAPHICAL ABSTRACT

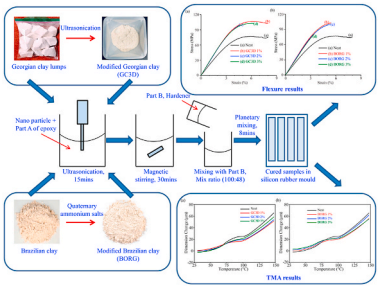

ARTICLE INFO

Keywords:
Biobased epoxy
Georgian clay
Bentonite clay
Mechanical properties
Sonochemical
Surface modification

ABSTRACT

This study focuses on the preparation and characterization of nanocomposite system with bio-based epoxy resin (Super SAP 100/1000, contains 37% bio-based carbon content) and natural clays including Georgian clay and Brazilian clay. Georgian clay was surface modified using an ultrasound processing in presence of Decalin. Brazilian clay was modified to organophilic bentonite using quaternary ammonium salts. The resulting nano clay particles were characterized using XRD and TEM to confirm the particle size reduction and uniform distribution. The as-fabricated nanocomposites were characterized using flexure, DMA, TMA and TGA. The flexure analysis showed that the modified clay composites have significant improvement in strength (23–38%) and modulus (28–37%). Delayed thermal degradation was observed from TGA analysis which showed that the major degradation temperatures improved from 7°-25°C. DMA and TMA analysis showed improvements in storage moduli (4–6%) and coefficient of thermal expansion (CTE) (6–64%), respectively. The notable improvement in thermal and mechanical properties suggested the effective dispersion and the high degree of polymer particle interaction. The bio based content present in the Super Sap 100/1000 acts as plasticizer resulting in the extensive ductility of the polymer.

1. Introduction

In view of the escalating environmental concerns and shrinking of petroleum resources, sustainable polymer nanocomposites have become the focus of interest for material scientists and engineers. Thus there is an increase in demand for bio-based polymers derived from natural

* Corresponding author.
E-mail address: vrangari@tuskegee.edu (V.K. Rangari).

https://doi.org/10.1016/j.matchemphys.2020.123821
Received 2 July 2020; Received in revised form 29 August 2020; Accepted 3 September 2020
Available online 16 September 2020

sources because of their inherent benefits such as biodegradability, reasonable cost, ease of access etc., [1]. Among thermosetting polymers, epoxy resins refer to a characteristic epoxide group represented by three membered ring known as oxirane or epoxy ring which are highly strained and reactive [2]. The molecular base of this epoxide group can be varied widely resulting in the diversity of molecular structure and thus various classes of epoxy resins. The chemical structure of the curing agents and the curing conditions influence the epoxy resins to achieve desirable properties for specific applications [3]. The epoxy resins have garnered substantial attention due to their intensive application in high performance coatings, castings and adhesives [3–5] with their versatile characteristics such as high strength and hardness [6,7], low shrinkage during cure, good impact resistance, and excellent electrical, chemical and heat resistance [4,8–10]. Despite the remarkable characteristics of epoxy resins, they suffer from high brittleness and low toughness [4,11]. Thus to further enhance and to obtain the desired properties of the epoxy resins, reinforcing them with various inorganic nanofillers has been very prevalent.

Owing to the increased surface area of interaction between the polymer matrix and nano filler, the mechanical, thermal, electrical/electronic and barrier properties and flammability resistance of the polymers can be substantially improved by addition of few fillers ($\leq$5%) such as clay or other nanoparticles [12–15]. Layered silicates (clays) have noteworthy effect on polymer composites. Their high intercalation chemistry leads to better interaction with the matrix, and thus enhance the properties of the resulting nanocomposites. Also, their high aspect ratio, ease of availability and low cost have made them to be one of the ideal nano reinforcements for polymers [2].

Natural clays are suitable candidates as fillers for their layered structure and high intercalation chemistry. They are widely available and are also cheap. Georgian clay, found in Georgia, USA, is a layered structure of kaolinite. Industrially, it is used in the production of pottery, cosmetics, and medicine. Georgian clay is very cheap. In addition to the cosmetic usage, consumption of White Dirt (another name for Georgian Clay) is very common in southern US, especially among African-American pregnant women [16].

Georgian clays are primarily composed of kaolinite. Kaolinite [$Al_2Si_2O_5(OH)_4$] is an important industrial raw material with numerous applications in ceramics, paper manufacturing, inks and paints, and in the production rubber and polymers [17–19]. The most important parameters to control the technical applicability of kaolinite are surface area, brightness, crystallinity, and particle size [20,21]. The mechanical strength, elastic modulus and thermal stability for the polymer composites were significantly improved when infused with kaolinite. Su et al. performed functionalization of kaolinite by silylation of 3-aminopropyltriethoxysilane onto the surface of ground kaolinite [22]. The functionalized kaolinite epoxy nanocomposites have shown improved storage modulus and glass transition temperatures compared to non-functionalized kaolinite composites. The silane treated halloysite nanotube (HNT) and layered double hydroxide (LDH) nanoclays were reinforced in epoxy resin system and the fire and mechanical properties were compared for the epoxy composites [23]. The silane treated HNT nanoclay has shown higher tensile and fire resistance properties compared to LDH. Cabedo et al. produced kaolinite nanoparticles with a combination of chemical and mechanical treatment [24]. First, the aqueous suspension of the clay was sieved followed by ultrasonication. Then the suspension was dried, milled and suspended in water/DMSO solution for three days with stirring at 50 °C. Part of the suspension was also diluted in methanol, and in, octadecylamine. Finally, all three suspensions were dried and milled in an agate mortar and developed ethylene-vinyl alcohol/kaolinite nanocomposites. They reported that the partial exfoliation and intercalation of the clay platelets was the dominant morphology attained. For clay loading below 8%, they reported an increase in thermal resistance, glass transition temperature, crystallinity, and barrier properties to oxygen. Zhang et al. worked with a novel biodegradable nanocomposite based on poly (3-hydroxybutyrate-*co*-3-hydroxyhexanoate) and silylated kaolinite/-silica core–shell nanoparticles [25]. With low loading of silane-modified kaolinite/silica core–shell nanoparticles, they reported increase in the tensile strength and toughness. Transmission electron microscopy (TEM) confirmed that filler material was finely distributed in the polymer matrix.

Although several methods were available for the synthesis of the clay minerals, sonochemical process has proved to be one of the most efficient techniques to generate the nanoparticles with the desired characteristics while retaining the crystalline structure [26–29]. Ultrasound processing made it possible for a lot of chemical reactions to occur those which may not be possible by any other means. The reason behind that is ultrasound is a physical phenomenon that can create the conditions necessary to drive chemical reactions. One of the most important of conditions exhibited by ultrasound processing is cavitation phenomenon-the formation, growth, and implosive collapse of bubbles in a liquid. The disintegration of the cavities thus formed results in production of massive energy causing the agglomerated particles to break down into tinier particles or the occurrence of the chemical reactions [30]. Ultrasound can produce a delamination effect in clay particles and the delaminated clay exfoliate in favorable polymer matrices [26]. The resulting composite thus have better structural integration in between the exfoliated clay and polymer matrix which resulted in improved thermal, mechanical and barrier properties [22,25,31–33]. Franco et al. modified the kaolinite with ultrasonication and studied its effect on the thermal behavior [34], and particle size and structural disorder [26]. Their findings are that the sonication can be manipulated to produce translation disorder and delamination effect, and to reduce particle size. Particle size reduction can be controlled by controlling different variables such as power of ultrasonic processor, amount of sample and time of the treatment. With the most energetic treatment for 20 h, they found that surface area got increased from 8.5 to 83 m^2/g, and the particle size got reduced.

Brazilian chocolate clay is another cheap clay available locally in Paraiba province of Brazil. The clay mainly contains bentonite which can also be used as a filler. Brazilian clays belong to smectite group of clays; they are poly-cationic, and they could be *trans*-formed into sodium bentonites [35]. They are composed of layers of two silica tetrahedral sheets with a central alumina octahedral sheet. The metallic ions occupying the interlayer space are predominantly Ca^{2+} ions and can be replaced with Na^{+}.

Valenzuela-Díaz et al. described the preparation of organophilic clays from Brazilian smectite clay [36–38]. They dispersed the clay in deionized water and sodium carbonate. After stirring the suspension for 30 min at 97 °C, quaternary ammonium salt - Arquad 2HT-75 and Arquad B50 was added at a concentration equivalent to 1.1 CEC of the clay. The suspension was then filtered, washed with deionized water, dried and stored at room temperature. Araújo et al. also prepared organophilic bentonite clay from the industrial bentonite sample which is originated from Boa Vista, PB, Brazil [39–42]. Bentonite clay was mixed with an aqueous solution of quaternary ammonium salt by mechanical stirring. The mixture was then washed several times with deionized water to remove excessive salts. Then the mixture was dried at 60 °C for 48 h and finally sieved in 200 mesh. Araújo et al. worked with the processing and characterization of polyethylene/Brazilian clay nanocomposites [40]. They used organically modified bentonite with four types of quaternary ammonium salts. They reported that all the quaternary ammonium salts were intercalated between two basal planes of the clay. They also reported improved thermal stability and flammability resistance. Furthermore, electron-beam treated HDPE composites reinforced with rice husk ash and the Brazilian clay showed great improvement in tensile, flexural and impact properties with a high cross-linking degree of 85% [43]. The thermal stability and fire behavior of organoclay filled PLA nanocomposites was enhanced due to the efficient dispersion and the compatibility between polymer and nanoparticles [44,45].

In the recent years epoxy/clay nanocomposites have been widely studied and are used in various applications such as tooling, laminates, molding castings and coatings [5]. However, driven by the need for lowering the global impact due to biodegradability, scientists are compelled to develop promising alternatives to recalcitrant petroleum based polymers. To-date, the inexplicable properties of bio-based epoxy nanocomposites with bio-based fillers are not yet completely unveiled. Hence, the current work focuses on the green material design where biodegradable epoxy nanocomposites are developed with comparable mechanical and thermal properties as of traditional ones.

In this work, we present the preparation and characterization of bio-based epoxy resin (Super SAP 100/1000, contains 37% bio-based carbon content) nanocomposites incorporated with bio-sourced, modified Georgian and Brazilian clay nanoparticles. The collected Georgian clay is subjected to ultrasonication to reduce the particle size. The Brazilian clay is modified using the quaternary ammonium salts. Thus obtained nano clay particles are then dispersed in biobased epoxy resin using ultrasonication and non-contact mixing to produce uniform dispersions and cured at room temperatures. The samples are then characterized for thermal and mechanical properties.

2. Materials and methods

2.1. Materials

A bio-based epoxy resin, Super Sap® 100/1000 with 37% bio-based carbon content epoxy was used for the development of polymer nanocomposites. This was a two-part epoxy resin with Part- A being Super Sap® 100 Epoxy, a modified, liquid epoxy resin and part B being Super Sap® 1000 Hardener. Super Sap® 100/1000 epoxy resin system was purchased from Entropy Resins Inc., San Antonio, CA. Unlike conventional epoxies, Super Sap® formulations contain bio renewable materials which are co-products from pine-based feedstocks or from waste streams of other industrial processes, such as wood pulp and bio-fuels production. The natural components results in excellent elongation and exceptionally high mechanical properties with good adhesion, fast room temperature cure cycle and good wettability [46]. This formulation has significantly contributed to the environmental factors by minimizing the carbon monoxide and greenhouse gas emissions to 50% and by elimination of harmful by-products and as such gained the United States Department of Agriculture (USDA) Bio Preferred℠ Product classification [47]. The performance and the processing data for Super Sap® 100/1000 epoxy resin system is shown in supplementary material in Table S1.

Georgian Clay, also known as White Clay was obtained locally. As the name implies, it was originated from Georgia, US. White clay mainly comprises of layers of Kaolinite. Georgian clay (white dirt) is Kaolin clay is widely used for medically to treat diarrhea, dysentery, cholera, and is also used in paper making, paint, fiberglass, porcelains and toothpaste. This is a high grade material. Some of the most popular products that have been made with kaolin (white dirt) are Kaopectate, Rolaids, Di-gel, Mylanta, and Maalox.

Brazilian Clay was received from Boa-Vista, PB, Brazil. This particular variation, which is found in abundance locally, is called chocolate clay, and is mainly comprised of sodium bentonite.

Brazilian Clay (Organophilic Bentonite) is also well known and we have modified following the published procedure [48]. The Brazilian clay (32 g) was dispersed in water (768 g) and kept under constant stirring. After 20 min an aqueous solution of the quaternary ammonium salt (20.4 g salt in 20 g water) was added and the resulting dispersion stirred for 20 min longer and left to rest at 25 °C for 24 h. The dispersion was filtered, washed with water and dried in an oven at 60 °C for 48 h. The treated clay was de-agglomerated with a mortar and pestle and sieved through 100 mm sieve before being used.

Decahydronaphthalene (Decalin), mixture of cis + trans with reagent grade 98% (Model no: MFCD00004130) is used for functionalizing nanoparticles using ultrasonication was obtained from Sigma Aldrich, St. Louis, MO. Denatured reagent grade ethanol (CH_3CH_2OH) used for washing the decalin and the precipitate was also purchased from Sigma Aldrich, St. Louis, MO.

2.2. Modification of nanoparticles

The collected lumps of Georgian clay were ground using agate mortar to obtain very fine powder (GCGD). The powder was then dispersed in decalin (50 ml for each gram of GCGD), and the solution was ultrasonicated for 3 h using 50% amplitude of 20 kHz vibration at the ½ inch probe tip. Ultrasonication was carried out using a Sonics vibra cell ultrasound, modeled as WCX 750. This unit consists of ultrasonic liquid processor of 750 W output with 20 kHz, 100 W/cm^2 converter and a flat titanium horn of 19 mm in diameter. After sonication, the solution was washed with ethanol and centrifuged at 5000 rpm for 5 min using Allegra 64R, Beckman Coulter Benchtop Centrifuge. After removal of the solvent, the precipitate was again washed with ethanol and centrifuged. This procedure was repeated until a clear solution over the precipitates was found. The ethanol was then decanted from the precipitate. The precipitate was then vacuum dried for 24 h to obtain the final nano-powdered white clay (GC3D).

The as collected Brazilian clay (BSOD) was characterized, and vacuum dried before use. The clay was modified by the addition of a quaternary salt and sodium carbonate and underwent the processes of dispersion into water, stirring and heating for a determinate time, and was filtered and dried for the disaggregation of one particle in another, and finally characterized. The modified Brazilian clay is obtained by following the synthesis procedure described by Ref. [49]. The nanoparticles that were obtained during the process were labeled along with their corresponding nanocomposites in Table 1.

2.3. Development of the nanocomposites

The clay nanoparticles were infused into the Super Sap® 100/1000 resin and the thermal and mechanical properties of thus obtained nanocomposites were evaluated. Firstly, about 100 g of part A of the epoxy was measured in a beaker and the nanopowder clay was added in 1, 2 and 3 wt% categorically. This mixture was ultrasonicated for 15 min using a 2:1 on-off cycle with 50% amplitude to prevent agglomeration of the particles using Sonics vibra cell ultrasound, WCX 750. Subsequently, the ultrasonicated mixture was magnetically stirred for 30–45 for uniform and effective dispersion of nanoparticles. Finally, the hardener, part B of the epoxy was added in a ratio of 100:48 for part-A and part-B for each of the specimens. The resulting mixture was then mixed (2000 rpm, 5 min) and defoamed (2200 rpm, 3 min) in a planetary non-contact mixer (Thinky mixer, ARE-250).

The mixture was then poured into silicon rubber molds (size compliant with ASTM standard) for flexure and DMA test. The mixture in silicon molds was then cured for 24 h s at controlled room temperature (25 °C) followed by post curing for 2 h at 48.9 °C in oven (Isotem 200 series-230 F). The specimens were then allowed to cool for 3 h at room temperature. The specimens thus obtained meets specific dimensions for characterization and were stored.

Table 1
Labels of nanoparticles and nanocomposites.

Nanoparticle	Description	Relevant Nanocomposite
GCGD	Georgian Clay, grounded by hand	SS/GCGD
GC3D	Georgian Clay, sonicated for 3 h in Decalin	SS/GC3D
BSOD	Brazilian Clay, Sodium Bentonite	SS/BSOD
BORG	Brazilian Clay, Organophilic Bentonite	SS/BORG

2.4. Experimentation of the nanocomposites

The nanoparticles characterized using X-ray Diffraction (XRD) and Transmission Electron Microscopy (TEM). For XRD, a Rigaku-DMAX-2000 X-ray diffractometer which is equipped with Cu Kα radiation (λ = 1.54 A°) was used at 40 KV and 30 mA, 5°/min scanning rate, and 0.020 sampling width from 3° to 80° of 2θ angles. A JOEL 2010 TEM unit was used to conduct transmission electron microscopy (TEM). Nanoparticles were first dispersed in ethanol and then 1 μL of the solution is dispensed on copper grid which was observed in TEM with an operating voltage of 80 kV.

The thermomechanical properties of the developed nanocomposites were analyzed using flexure, TGA, DSC, TMA, and DMA analysis. Epoxy composites are mostly used for structural applications such as laminates and tooling. Hence, it is important to understand the mechanical behavior of such epoxy composites. The flexure properties of the developed nanocomposites were evaluated by three-point bend loading. The flexure test was followed according to ASTM D790 – 10 procedure B [50]. Flexure test specimens with span to thickness ratio (l/d) of 16, with the dimensions as 90 × 12 × 4.5 mm were studied. The span support length of the specimen is 72 mm. A Zwick/Roell Z2.5 materials testing system with 2.5 kN load cell which consists of TestXpert data acquisition system was used for flexure test. Strain rate of 20 mm/mm/sec and cross head speed of 1.6 mm/min were considered for conducting flexure test. Five specimens were tested for each of the mechanical tests and the average of the results was considered.

The fracture surface of the specimens that underwent flexure analysis were analyzed using scanning electron microscopy (SEM). A JEOL JSM-5800 SEM was used to perform microstructural analysis. The specimens were coated with gold/palladium (Au/Pd) for 5 min at 10 mA, 5 V and 20 millitorrs using Hummer 6.2 sputter coater system purged with Argon gas.

Thermogravimetric analysis (TGA) was carried out using a thermogravimetric analyzer, Q-500 from TA Instruments. Approximately 12 mg were cut from the specimens and were loaded in platinum sample pan. The samples were heated up to 650 °C ramped at 5 °C/min in nitrogen environment (60 mL/min). TA Universal Analysis software is used to analyze the data that is obtained from the TA instruments.

For differential scanning calorimetry (DSC), a differential scanning calorimeter, Mettler Toledo was used to analyze thermal properties of the specimens. Approximately 10 mg–12 mg of the samples were cut from the developed nanocomposite specimens and were sealed in aluminum pans for testing. Each sample was heated up to 200 °C with a heating rate of 5 °C/min in nitrogen environment (60 mL/min).

Thermomechanical analysis (TMA) was carried out using Q-400 from TA Instruments in expansion mode. Specimens of dimensions 90 × 12 × 4.5 mm were considered and were subjected to constant probe force of 0.2 N with a heating rate of 5 °C/min up to 150 °C in nitrogen environment (50 mL/min) following ASTM D696 - 08 standards [51]. Coefficient of thermal expansion (CTE) was determined from this test by evaluating the ratio of change in length of the specimen due to heating or cooling per unit length of the specimen and the change in the temperature [51]. The CTEs were evaluated in the ranges of 30–70 °C and 110–140 °C using TA Universal Analysis software.

For dynamic mechanical analysis (DMA), a dynamic mechanical analyzer, Q-800 from TA Instruments purged with nitrogen gas (50 mL/min) was used with a heating rate of 5 °C/min up from 30 °C to 150 °C. The mode of loading was double cantilever with a vibration frequency of 1 Hz for the specimens of dimensions 35 × 14 × 4.5 mm.

3. Results and DISCUSSION

3.1. Characterization of Georgian Clay

The as received Georgian clay was hand ground to obtain a fine powder. Fig. 1(a) shows the X-ray diffraction pattern of the ground Georgian clay (GCGD). The pattern suggests that the Georgian clay is highly crystalline, and it is similar to kaolinite – Al2(Si2O5)(OH)4 (JCPDS-Pdf #78–1996). Kaolinite has a layered silicate structure. Crystalline Kaolinite particle sizes are estimated from the X-ray pattern using full-width-half-maxima (FWHM) method and Debye-Scherrer formula. The estimated crystallite size from the 100% peak of the X-ray pattern of (001) plane was found to be 28.4 nm.

Ultrasonic irradiation using a low vapor pressure solvent (Decalin) can create high temperature and pressure conditions which are responsible for chemical oxidation and reduction reactions [52]. Ultrasonication generates bubbles that get bigger, as a result of the vapor pressure difference. As more power is introduced, the bubbles get enlarged. Finally, the bubbles collapse and that create enormous local heat (temperature >5000 K), pressure (>20 MPa) and high cooling rate (>107 K/s). This localized effect leads to the breaking of the solute particles into smaller sizes and can cause much structural and chemical change in the resulting particles. Fig. 1(b) shows the X-ray diffraction pattern of the ultrasonicated Georgian clay (GC3D). Sonication did not cause any kind of amorphization in the clay structure. The structure is still kaolinite. However, ultrasonication caused the X-ray peak widening, which suggests the particle size reduction. Particle sizes were calculated using the FWHM method and Debye-Scherrer formula from the 100% peak of the x-ray pattern at (001) lattice plane. The estimated crystallite sizes were found to be 20 nm.

Layered clays show another significant effect that can be triggered by ultrasonication which is the expansion of the clay layers. With suitable solvent and reaction environment, the organic cation from the precursor can replace the exchangeable cations that are present in between the silicate layers. Cavitation - the formation, growth, and implosive collapse of bubbles in ultrasonication with a low vapor pressure solvent can lead to such a result. In this experiment, the organic cation of Decalin can be exchanged with the ions in between silicate layers of kaolinite and thus can expand interlayer space which might have resulted in the increase of d-spacing (See Supplementary Fig. S1). This expanded clay structure is useful for the clay to be used as a filler in the polymer matrix as it allows favorable diffusion of polymer in between the interlayer spacing [2]. As such, the enhanced dispersion ability of clay materials with nano thickness of individual layers, high aspect ratio and large surface area facilitates the improved thermal, optical, barrier as well as mechanical properties of the polymer nanocomposite [53,54].

Expansion of d-spacing of such clay structure is verifiable from the x-ray diffraction pattern of the resulting particles. Fig. 1(c) and (d) show the x-ray diffraction pattern of the Georgian clay before (GCGD) and after the ultrasonication (GC3D) in the low Bragg angle zone (5–15°). As evident from the figure, ultrasonication has caused the clay to be slightly expanded. For the as it is clay (GCGD), the peak from the (001) lattice plane occurs at the Bragg angle of 12.460° with a d-spacing of 7.0978 Å. After modification with ultrasound (GC3D), the peak shifted to a Bragg angle of 12.320° with d-spacing of 7.1875 Å. Thus, the (001) plane is expanded by about 0.1 Å. Also the peak of GCGD at 2θ = 9.060° and 9.7525 Å d-spacing is expanded to 2θ = 8.817° and 10.0207 Å after modification. This plane is expanded by about 0.3 Å. The expansion of kaolinite layers clearly indicates that ultrasonication in the presence of Decalin has organically modified the Georgian clay. Earlier researchers have reported intercalation/exfoliation with modification of kaolinite with other solvents and have found similar increment of d-spacing [55–57]. However, depending on the solvents and other precursors, and the operating, working, and experimental condition, the actual amount of d-spacing expansion varies.

Particle size, shape and distribution of the Georgian clay both before and after the ultrasonication were examined by TEM. Fig. 2(a) shows the TEM image of the as received Georgian clay. As seen from the micrograph, the particles are highly agglomerated. Furthermore, the size of the platelets is observed to be higher compared to the crystallite size obtained from XRD. The discrepancy in the size might be due to the structure of clay particles which are in the form of platelets. The FWHM

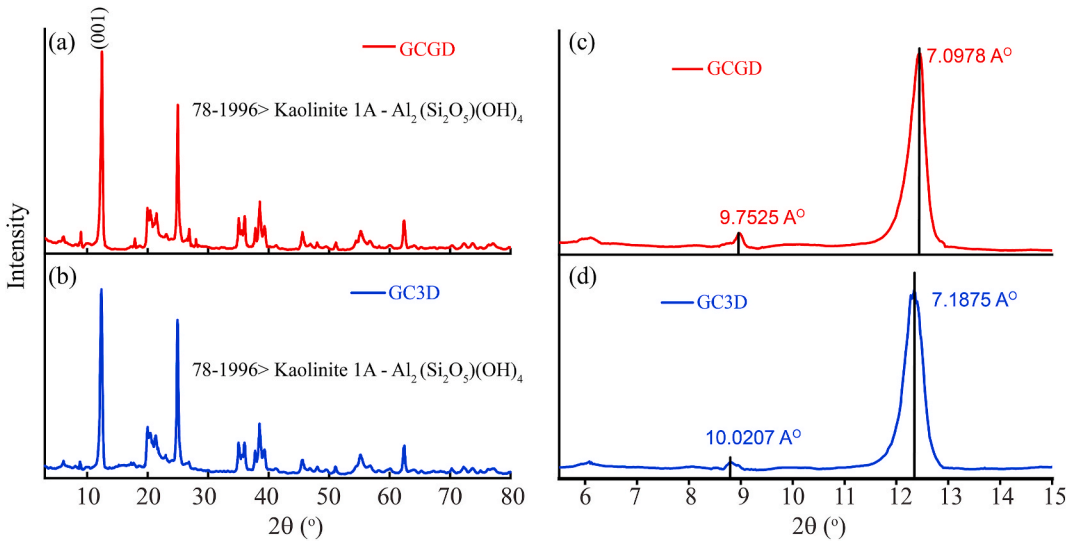

Fig. 1. X-ray diffraction pattern of (a) ground (GCGD) and (b) ultrasonicated (GC3D) Georgian clay; d-spacing expansion of (c) ground (GCGD) and (d) ultrasonicated (GC3D) Georgian clay.

method and Debye-Scherrer formula are efficient for calculating the crystallite sizes which are spherical in shape. The higher resolution version of the as received Georgian clay (Fig. 2(b)) suggests that the clay has a layered structure. The micrographs clearly show the individual platelets of the clay. However, the platelets are irregular in their size and shape. Ultrasonication breaks the agglomerated nanoplates into further smaller size (Fig. 2(c)) with the layered structure of kaolinite thus promoting exfoliation. The size and shape of the individual layers are much more regular after sonication. The higher resolution version, Fig. 2(d), also reveals the layered structure.

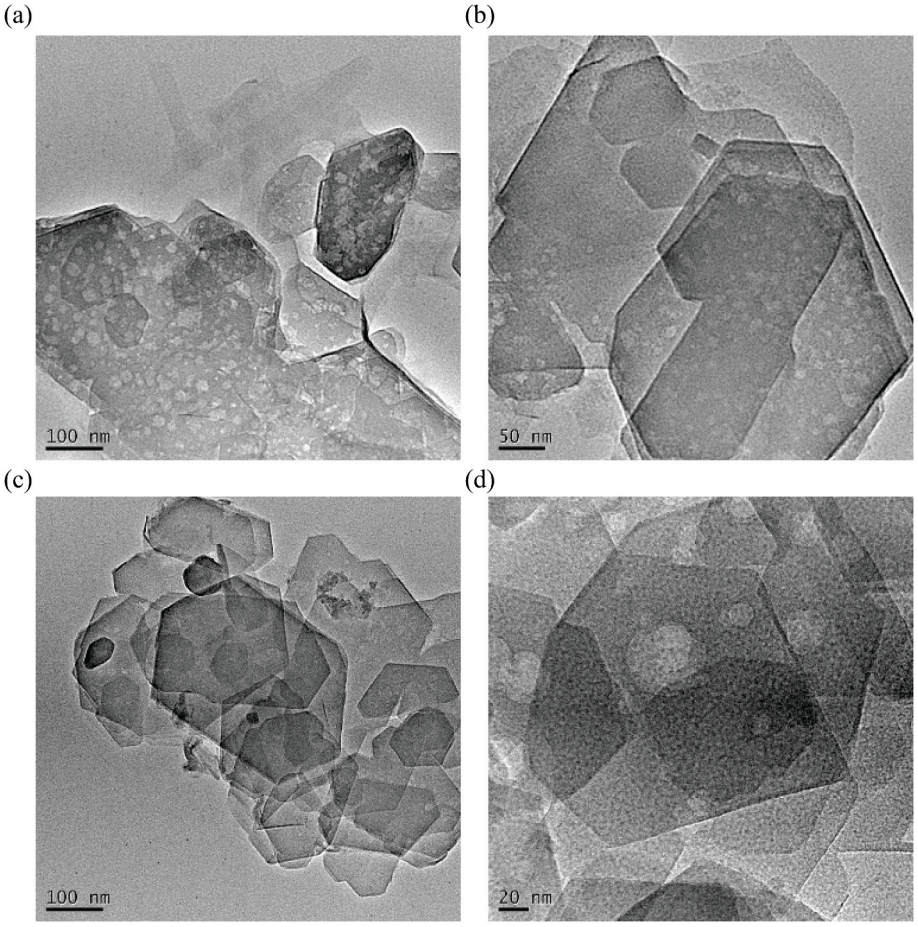

Fig. 2. TEM micrographs of Georgian clay (a) before sonication (GCGD), (b) expanded view of GCGD, (c) after ultrasonic modification (GC3D) and (d) expanded view of GC3D.

3.2. Characterization of the Brazilian Clay

Brazilian clays are smectite clays. The as received Brazilian clay was sodium bentonite clay. It contains mostly Na^+ cation in between the smectite layers. Fig. 3(a) shows the X-ray diffraction pattern of sodium bentonite clay (BSOD). As shown from the pattern, Brazilian clay is purely crystalline. However, the x-ray pattern did not match with JCPDS database. The crystallite sizes of the clay were determined using Debye-Scherrer formula and FWHM method from the 100% peak of the pattern. The estimated crystallite sizes were found to be 71.6 nm.

Brazilian clay was modified with quaternary ammonium salts. The modified clay is also characterized for x-ray diffraction, and the x-ray pattern is shown in Fig. 3(b) which shows that the clay is crystalline after modification. However, the 100% peak of the pattern is widened, suggesting that the particle size is changed. The estimated particle size of modified clay was determined using Debye-Scherrer formula and FWHM method, and it was found to be 43.3 nm.

Modification of the Brazilian clay resulted in the entrapment of the quaternary ammonium organic cation in between layers of the bentonite clay. The polyatomic organic cation actually replaced the exchangeable Na^+ and other cations in between the layers [38,58–60]. This has resulted in the expansion of the clay structure. The expansion of the clay structure is evident from the change in d-spacing of particular planes in the x-ray pattern. As seen from Fig. 3, the first peak of sodium bentonite is found at a Bragg angle, $2\theta = 6.700^\circ$ and d-spacing of 13.1817 Å. However, this peak has shifted to Bragg angle, $2\theta = 4.739^\circ$ and 18.6323 Å d-spacing after organophilic modification with quaternary salts. This has caused an overall d-spacing expansion of 5.4506 Å. This significant amount of d-spacing expansion suggests that the Brazilian clay will follow the intercalated or exfoliated nanocomposites model while being used as a filler. Thus, modified Brazilian clay will have better interaction with the polymer in a nanocomposite system compared to the unmodified clay [61]. Earlier researchers who reported intercalation/exfoliation of the fillers in nanocomposites [36,62] have also found similar expansion of d-spacing for both Montmorillonite and Bentonite clays – the two clays are similar in their structure and belongs to the same smectite group of clay minerals [35].

In this study, the maximum expansion of the Georgian clay is found around 0.1 Å when ultrasonicated in the presence of decalin. For the Brazilian clay, the expansion is around 5.5 Å. It is to be noted that the modification of Brazilian clay was done with quaternary ammonium salt in an experimental condition that leads to a chemical reaction between the precursors. This has resulted in an increased interspacing distance between the clay layers. Whereas, Georgian clay is modified by simple sonochemical technique where decalin is used for functionalization.

The size, shape and distribution of the particles and the structure of the Brazilian clay were observed by TEM. Fig. 4(a) shows the TEM image of the as received Brazilian clay, sodium bentonite (BSOD). The particles are highly agglomerated; their size and shapes are much irregular. The crystalline structure of sodium bentonite is evident in the higher magnification version in Fig. 4(b). It also shows the layered structure of the Brazilian clay. Fig. 4(c) shows the TEM micrographs of the organophilic Brazilian clay. The micrograph clearly indicates the absence of particle agglomeration. The particle size is reduced below 50 nm, and the distribution of particle size is also even. The layered structure of the organophilic bentonite is also evident. Fig. 4(d) reveals that organophilic clays are also crystalline. It also confirms the particle size reduction.

3.3. Characterization of the nanocomposites

3.3.1. Flexural analysis

Three point bending test (flexure test) is used to evaluate the flexural properties like strength and modulus of all nanocomposite systems according to the ASTM standard D790. The flexural behavior of the Super Sap 100/1000 epoxy resin incorporated with ground Georgian clay (SS/GCGD), ultrasonicated Georgian clay (SS/GC3D), as received Brazilian clay (SS/BSOD) and organically modified Brazilian clay (SS/BORG) nanocomposite systems for 1%, 2% and 3% filler loadings are shown in Fig. 5(a–d), respectively.

Table 2 summarizes the flexural properties of the Georgian clay and Brazilian clay filled nanocomposite systems. The results in Table 2 show that the maximum flexural strength is found for 1% filler loading of the GC3D, and the maximum flexural modulus is found for 2% filler loading of the same. Thus, flexural strength is improved up to 37.64%, and the modulus is improved up to 37.05%. For BORG clay loading, the

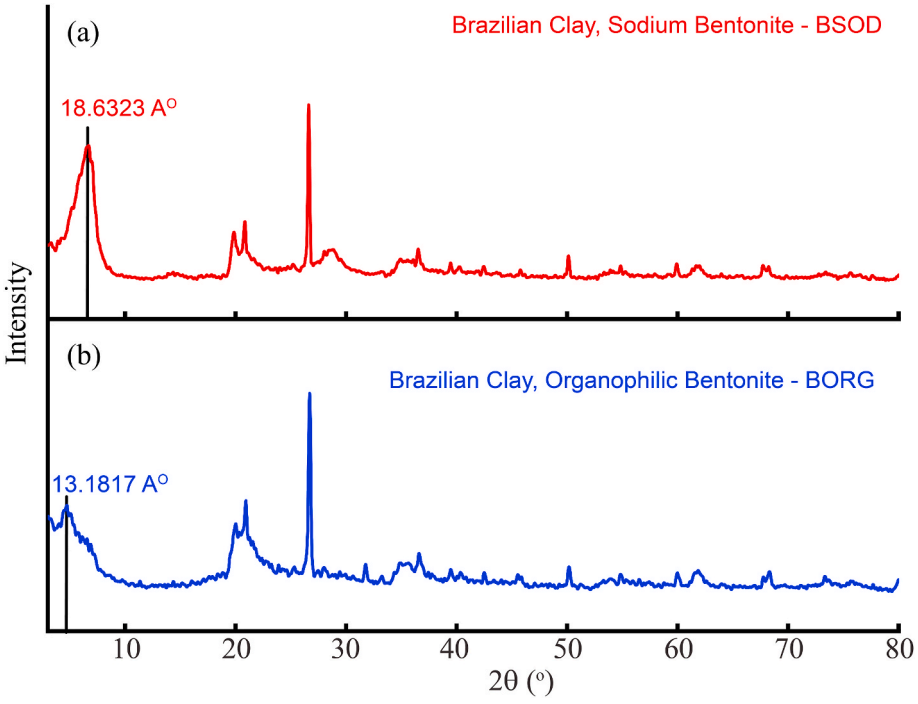

Fig. 3. X-ray diffraction pattern of (a) sodium bentonite- BSOD and (b) organophilic bentonite- BORG.

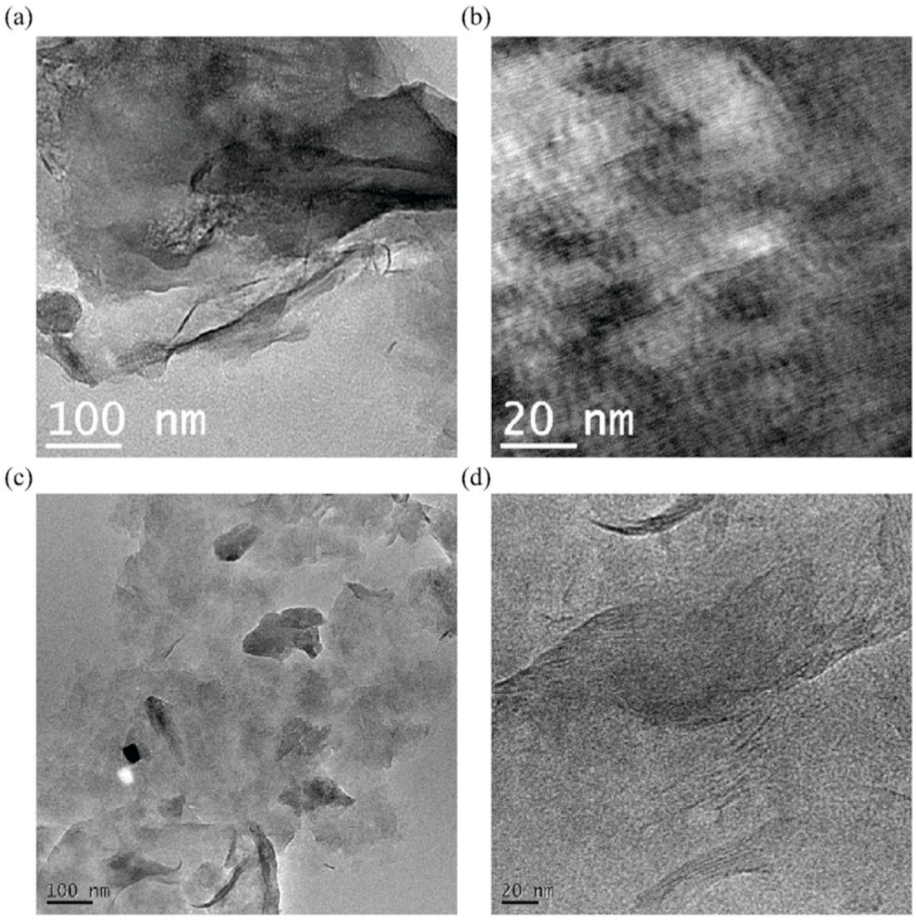

Fig. 4. TEM micrographs of Brazilian clay (a) sodium bentonite (BSOD), (b) expanded view of BSOD, (c) organophilic bentonite (BORG) and (d) expanded view of BORG.

maximum flexural strength is found for 1% loading of BORG, and the maximum flexural modulus is found for 2% loading of the same which shows an improvement in flexural strength up to 33.13% and in flexural modulus up to 30.25%. Prakash et al. [63] reported that 3 wt% of Kaolin reinforced epoxy has highest flexural strength of 73.325 MPa for crosshead speed of 7 mm/min when compared with 0–7.5 wt% for crosshead speeds of 3, 5 and 7 mm/min. Zhou et al. [64] reported 13.5% improvement in flexural strength for 1–4% of montmorillonite clay loaded carbon/epoxy composites. Whereas, Singh et al. [65] showed that when montmorillonite clay is dispersed in epoxy by hand mixing and ultrasonication, there is 32.9% improvement in flexural modulus compared to the neat epoxy. These results comply with the present findings in the study.

For both Georgian and Brazilian clay filled nanocomposites, the flexural properties for the modified clay filled nanocomposites (SS/GC3D and SS/BORG) has shown greater improvement compared to unmodified clay composites (SS/GCGD AND SS/BSOD). The flexural strength and modulus has increased for all the variations of clay filled nanocomposites compared to the neat epoxy system subjected to the same processing and testing environment. However, for most of the nanocomposites, the strain at maximum stress is not much changed. This behavior suggests that the ductile behavior of Super Sap 100/1000 epoxy polymer is not influenced much with the addition of nanoparticles as filler [66]. This is particularly interesting, because it suggests that the structural interaction between fillers and the matrix has only influenced to improve the flexural strength and modulus of the nanocomposites. Hence, the particles and matrix interaction was due to the physical effect of filler addition and there was no crosslinking or chemical bonding between them [67,68]. The enhancement of the flexural properties for SS/GC3D is partly attributed to the decrease in the particle sizes of the clay after ultrasonication, which in turn has increased the surface area of the nanoparticles. This has resulted in increased interaction in filler-polymer interface and thus has improved flexural properties. Also, the particle size distribution being more even may have caused better dispersion of the clay as filler in the polymer matrix. As evident from the TEM micrographs of GC3D (Fig. 2(d)), ultrasonication has also produced the expanded layer effect on the clay. The clay layers are thus more separated. Provided that, exfoliated layered clays act as separate particles, and thus lead to good dispersion of the fillers [69]. There was also a slight increase in d-spacing in the clay structure as evident from the X-ray pattern (Fig. 1). On the other hand, the TEM micrographs of the BORG (Fig. 4(d)) also has suggested that particle size distribution is more even which has had caused better dispersion of the clay as filler in the polymer matrix. Most importantly, there is also an increase in d-spacing in the clay structure as evident from the X-ray pattern (Fig. 3) which suggests the reduction in particle size and expanded clay structure.

Overall, the particle size reduction as well as the expanded clay structure might have resulted in better interaction between the clay and the matrix [70]. Owing to these effects, the interaction between the polymer and clay might have increased which resulted in the improved material's resistance to mechanical loading in flexural test.

Fig. 6 shows the SEM micrographs of the fracture surfaces for the flexural analysis of SS/Neat, SS/GC3D (1 wt%) and SS/BORG (1 wt%) along failure plane. The fracture surface of the neat epoxy system is smooth and does not show any intricate features as shown in Fig. 6(a). Uninterrupted crack propagations were observed in smooth vertical paths along the thickness direction. The fracture surface suggests a

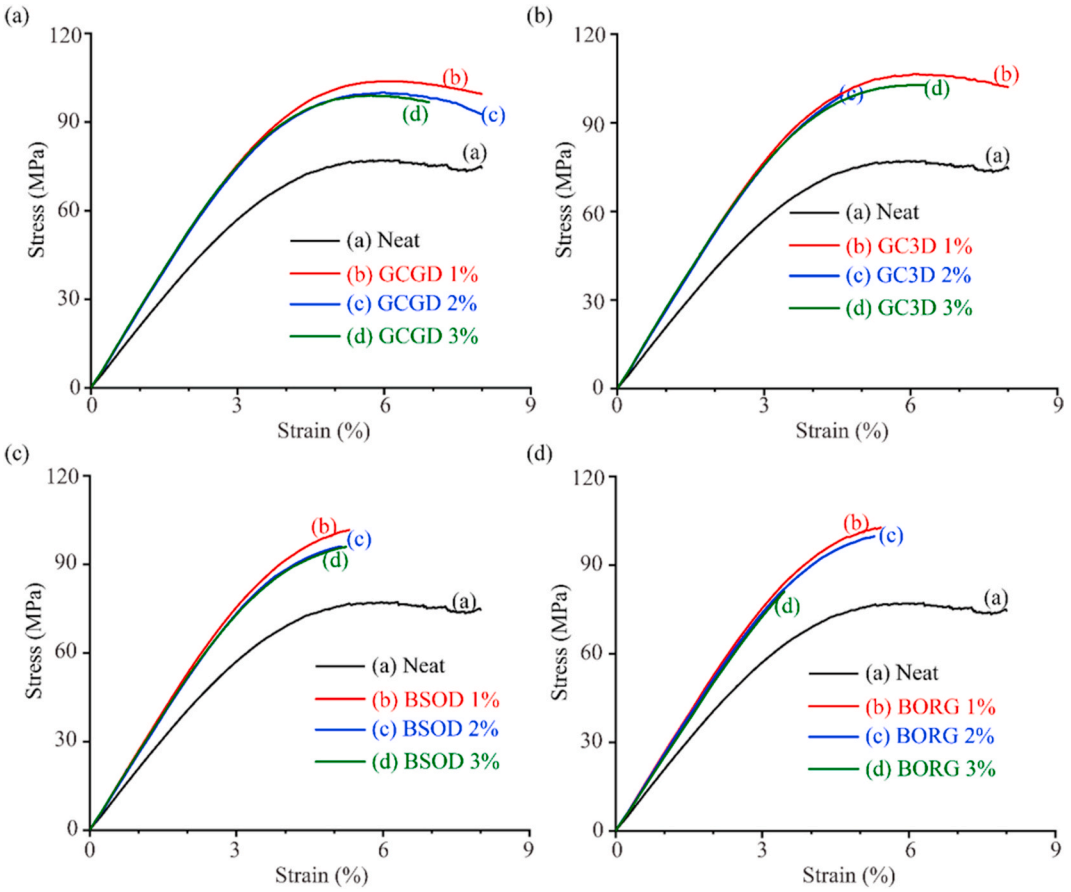

Fig. 5. Flexure behavior of the nanocomposites (a) SS/GCGD and (b) SS/GC3D (c) SS/BSOD and (d) SS/BORG with 1, 2 and 3 filler percentage.

Table 2
Flexural properties for the Georgian clay based nanoparticles filled composites.

	Filler Amount (wt.%)	Strain at Max. Stress (%)	Max. Stress (MPa)	Flexure Modulus (GPa)	Increase in Strength (%)	Increase in Modulus (%)
SS/Neat	0	6.05 ± 0.27	77.48 ± 3.14	1.95 ± 0.06	0.00%	0.00%
SS/GCGD	1	6.12 ± 0.13	103.97 ± 2.13	2.49 ± 0.15	34.19%	27.79%
SS/GCGD	2	5.93 ± 0.08	100.11 ± 2.88	2.40 ± 0.14	29.20%	23.08%
SS/GCGD	3	5.68 ± 0.29	99.29 ± 4.81	2.50 ± 0.17	28.15%	28.21%
SS/GC3D	1	6.30 ± 0.21	106.64 ± 2.14	2.51 ± 0.06	37.64%	28.72%
SS/GC3D	2	5.08 ± 0.91	103.05 ± 3.21	2.67 ± 0.13	33.00%	37.05%
SS/GC3D	3	6.16 ± 0.13	102.92 ± 1.5	2.53 ± 0.05	32.83%	29.95%
SS/BSOD	1	5.92 ± 0.55	103.01 ± 4.07	2.49 ± 0.16	32.95%	27.69%
SS/BSOD	2	5.46 ± 0.44	96.71 ± 7.79	2.43 ± 0.36	24.82%	24.36%
SS/BSOD	3	5.4 ± 0.11	96.3 ± 5.77	2.5 ± 0.39	24.29%	28.21%
SS/BORG	1	5.63 ± 0.22	103.15 ± 0.9	2.51 ± 0.15	33.13%	28.72%
SS/BORG	2	4.8 ± 0.69	97.48 ± 3.15	2.54 ± 2.54	25.81%	30.25%
SS/BORG	3	4.21 ± 0.06	95.32 ± 1.87	2.5 ± 0.04	23.03%	28.21

brittle fracture as the crack propagation is incessant. The fracture surface of SS/GC3D nanocomposite system with 1 wt% of filler which exhibits highest increase in strength is shown in Fig. 6(b). The surface of the SS/GC3D system is rough with wavy texture which indicates the increase in strength due to the interfacial bonding strength between the nanoparticles and the polymers [71]. Additionally, this also implies the improved ductility of the system. No visible voids and particle agglomerations were found on the surface suggesting the effective dispersion of the nanoparticles. The cracks were present all over the surface. The crack propagates along the ridge patterns and the wavy textures delaying the failure of the specimen, thus exhibiting the improved strength of the composite. On the other hand, the surface of the SS/BORG nanocomposite system with 1 wt% filler exhibits cavities. Voids localize the stress concentration resulting in the premature failure of the material [72]. Hence, the strength of the system deteriorates compared to that of SS/GC3D.

3.3.2. *Thermogravimetric analysis*

Thermal stability of the nanopowdered clay infused composite systems is analyzed using thermogravimetric analysis (TGA). Fig. 7(a) and (b) show the TGA weight loss and derivative weight loss curves of SS/GC3D and SS/BORG with 1%, 2% and 3% of filler loading, respectively. Both the onset temperature and the major degradation temperature of SS/GC3D and SS/BORG were improved as compared to SS-Neat. Thus, the thermal stability of the nanocomposite was improved.

TGA thermographs of the nano clay filled nanocomposite systems showed degradation at two different temperatures. The first one is at around 200 °C, which is a minor degradation and the major degradation

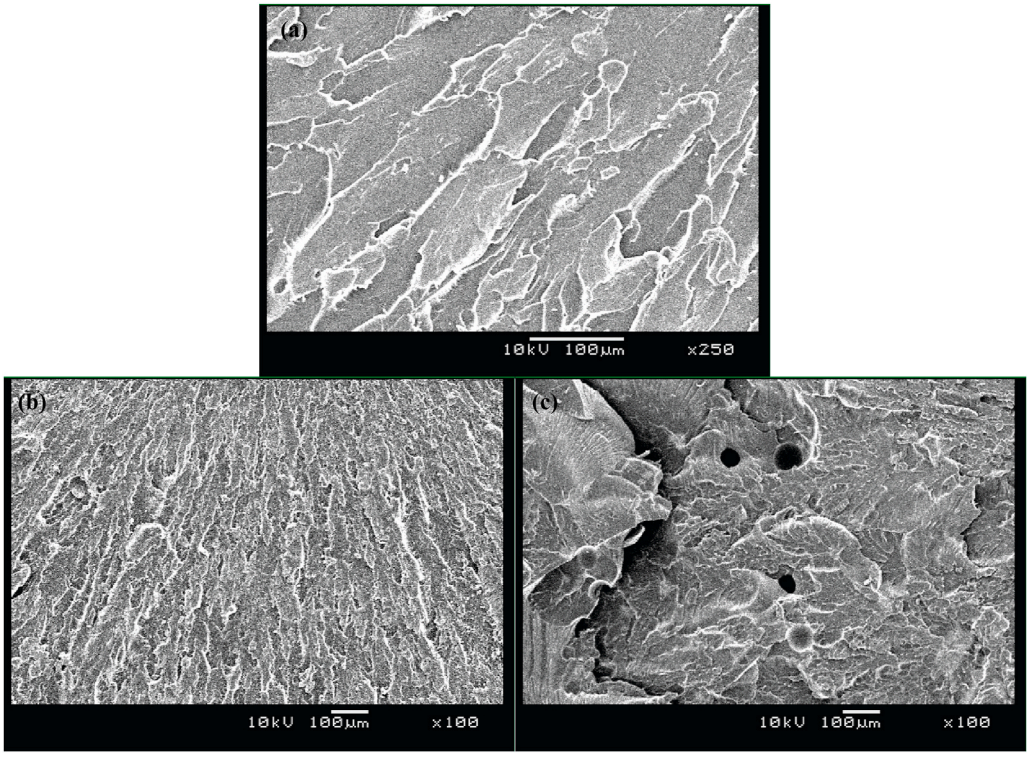

Fig. 6. SEM micrograghraphs of fracture surfaces of (a)SS/Neat (b) SS/GC3D for 1 wt% and (c) SS/BORG for 1 wt%.

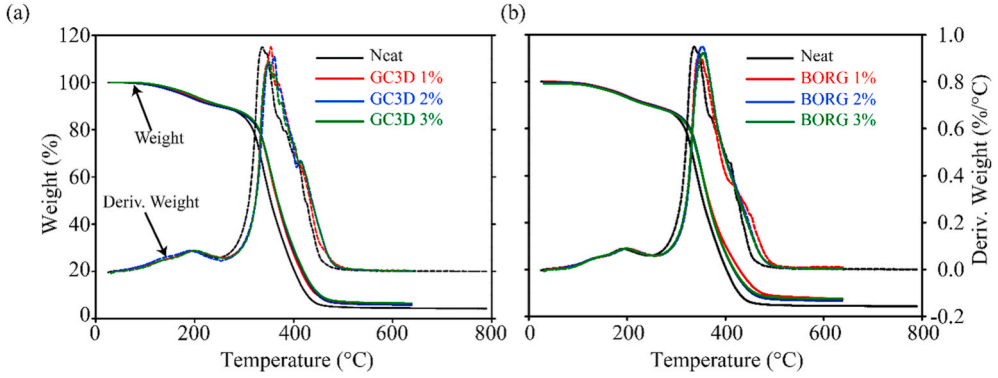

Fig. 7. TGA thermographs of (a) SS/GC3D and (b) SS/BORG nanocomposites.

has occurred at around 350 °C. The first degradation can be assigned to the decomposition of bio-based content of the Super Sap 100/1000 epoxy polymer [66,73,74]. The major degradation is attributed to the remaining petroleum-based content in Super Sap 100/1000 epoxy polymer.

Table 3 summarizes the TGA data of all the nanocomposite systems with Georgian clay and Brazilian clay at 1%, 2%, and 3% of filler loading. The improvement in onset (10–13 °C) and major degradation temperatures (7–25 °C) suggests that the nanocomposites are thermally more stable than the neat system, SS/Neat. Furthermore, the amount of residue left has increased compared to the neat epoxy system suggesting the improvement of fire retardant ability for the composite. Table 3 shows that the SS/GC3D composite with 2% filler loading has the highest onset temperature and major degradations temperatures which were improved by 13 °C and 25 °C compared to the SS/Neat system, respectively. Zhou et al. [64] reported 6 °C increase in decomposition temperature for 2 wt% clay modified carbon/epoxy composite. For Kaolinite reinforced in epoxy resin nanocomposite systems, Su et al. found that temperature at 5% weight loss decreased with the Koalinite

Table 3
Summary of Thermogravimetric analysis.

	Filler %	Onset Point (°C)	Major Degradation (°C)	Residue Left (%)
SS-Neat	0	315.51	335.72	4.364
SS/ GC3D	1	328.49	353.86	6.108
SS/ GC3D	2	328.8	360.96	5.759
SS/ GC3D	3	327	350.71	6.577
SS/ BORG	1	325.97	343.11	7.349
SS/ BORG	2	326.74	352.85	6.681
SS/ BORG	3	327.89	354.61	7.433

loading. These results suggest that the findings in the present study have shown in significant enhancement in thermal properties.

The weight loss progression is alleviated due to the presence of clay particles suggesting that the exfoliated clay enhances the thermal stability [75]. The nanoclay particles infused in the composite systems retard the thermal degradation by formation of incombustible and insulating char [74]. Formation of char at the initial stages results in the imperviousness of the volatile components that favors the decomposition. Furthermore, the layers of the clay act as a mass transport barrier to the volatile products generated during decomposition and thus impede the emission of the gaseous degradation products [2]. This suggests that the nanostructure of clay plays an important role in improvising the thermal stability of the nanocomposite. The nano clay particles hinder the evaporation of the small molecules generated in the thermal decomposition limiting the continuous decomposition of the polymer matrix [76]. This mechanism is shown to be effective in both Georgian and Brazilian clay filled nanocomposites.

3.3.3. Differential scanning calorimetry

The DSC heating curves of SS/GC3D and SS/BORG with 1%, 2%, and 3% loading of the filler is shown in Fig. 8(a) and (b), respectively. The onset and the glass transition (T_g) temperatures of SS/GC3D and SS/BORG have slightly decreased compared to SS/Neat with the reinforcement of nano clay particles. Similar observations were found in the literature [11,70,77,78]. The overall cure behavior of the Super Sap 100/1000 epoxy remains unaltered for the composite systems infused with nanoclay particles.

The endothermic reactions that were present in the temperature range of 50–60 °C in Fig. 8 might be due to the melting or similar phase change of bio based content which also showed the minor decomposition in Fig. 7. This bio-based content most likely acts as a plasticizer [77], which are small molecule chains that prevent any cross linking between the polymer due to the presence of filler materials. The bio-based content thus increases the plasticity (ductility) of the polymer. In addition to that, the presence of the exfoliated nano clay particles in the epoxy might have restricted the motion of the polymer chains in the epoxy network which resulted in the non-improvement of the glass transition temperature [11]. Hence, the enhanced mechanical and thermal properties of the nanocomposite systems might be due to the effective particle dispersion in the polymer matrix rather than the polymer cross linking.

3.3.4. Thermomechanical analysis

The dimensional stability of the nanocomposites infused with clay fillers were studied by comparing the coefficient of thermal expansion (CTE) in thermomechanical analysis (TMA) using the expansion mode. The dimensional stability is evaluated from the slope of the curves both before (30° - 70 °C) and after (110° - 140 °C) T_g. Fig. 9(a) shows the dimensional change of the Georgian clay filled nanocomposites, SS/GC3D, with temperature for varying (1%, 2% and 3%) filler percentages and Fig. 9(b) shows the TMA curves of SS/BORG. The CTE of both the composites is lowered before and after T_g as compared to SS/Neat. Thus, the overall dimensional stability of SS/GCGD and SS/BORG has improved. However, T_g has not changed significantly.

Table 4 summarizes the TMA behavior of the nanocomposites. The CTE of the nanocomposites, irrespective of the filler content decreased up to 64% before T_g compared to the neat polymer. The CTE after Tg has also improved up to 15%. The maximum improvement in terms of dimensional stability is found for 3% loading of BORG in SS/BORG. However, the improvement for 2% filler in SS/GC3D is also worth noting. For the epoxy systems filled with seven different fillers with 50 wt%, the CTEs decreased from 7% to 38% [79]. Su et al. [22] found that with the infusion of modified Kaolinite in the epoxy system, the CTE values decreased with the increase in the clay content. The findings from the present study yielded satisfactory results with the low amount of filler loadings whereas higher amount of loadings might result in the agglomeration of particles which deteriorates the mechanical properties [71]. The extent of CTE reduction might be due to the particle rigidity, dispersion of clay in the matrix, and efficient stress transfer to the clay layers. The inorganic fillers being stiffer compared to the matrix, are resistant to deformation and as such decreases the overall strain of the matrix leading to the increased dimensional stability [71]. In addition to that, the retardation of the chain movement in a clay filled nanocomposite can also benefit the decrement of CTE.

3.3.5. Dynamic mechanical analysis

The viscoelastic behavior of the nanocomposites is analyzed using dynamic mechanical analysis (DMA). DMA curves for the Georgian clay filled nanocomposites, SS/GC3D, are shown in Fig. 10(a). The storage modulus was improved for both 2% and 3% of filler loading whereas loss modulus was improved for all percentages of filler loading. The T_g of the nanocomposite, both by tan delta and loss modulus is not improved (See Supplementary Material Table S2). However, the change in T_g is not significant. Maximum improvement for the storage modulus (6.42%) is obtained for 2% of the GC3D clay loading in the nanocomposite. Improvement in loss modulus (7.09%) is highest for 3% of clay loading. Zhou et al. [64] found significant improvement of 58% in storage modulus for 2 wt% clay loading in epoxy composite. Su et al. [22] reported about 24.5% increase in the storage modulus for the modified Kaolinite infused epoxy composite when compared to the pure epoxy.

Fig. 10(b) summarizes the viscoelastic properties of the Brazilian clay filled nanocomposites, SS/BORG. Change in the properties is recorded for different filler percentage variation. The filler loading of 1% exhibited improvement in both storage (3.64%) and loss (3.87%) moduli.

The mechanical properties and the thermal stability of the filler

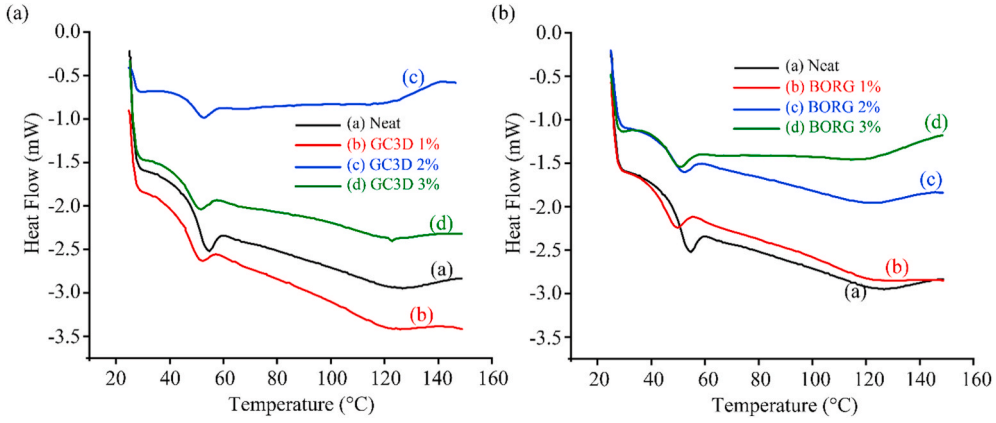

Fig. 8. DSC endotherms of (a) SS/GC3D and (b) SS/BORG nanocomposites.

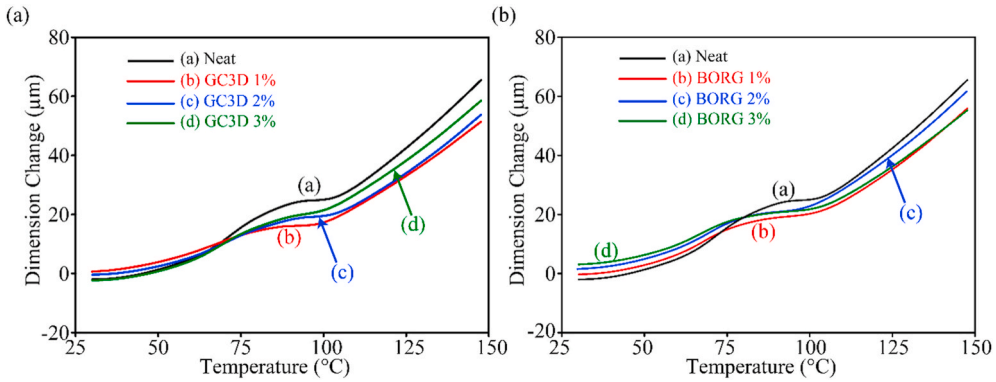

Fig. 9. TMA curves of the nanocomposites: (a) SS/GC3D and (b) SS/BORG.

Table 4
Summary of thermomechanical analysis.

	Filler %	CTE before T_g (µm/°C)	Change (%)	First onset point (°C)	Second onset point (°C)	CTE after T_g (µm/°C)	Change (%)
SS-Neat		0.8145	0%	85.52	104.36	0.9384	0%
SS/GC3D	1	0.4028	51%	82.35	100.31	0.8566	9%
SS/GC3D	2	0.3039	63%	83.17	103.79	0.8128	13%
SS/GC3D	3	0.3314	59%	81.02	102.22	0.7958	15%
SS/BORG	1	0.3193	61%	78	103.47	0.847	10%
SS/BORG	2	0.4093	50%	78.38	99.77	0.8784	6%
SS/BORG	3	0.2909	64%	81.43	105.45	0.8793	6%

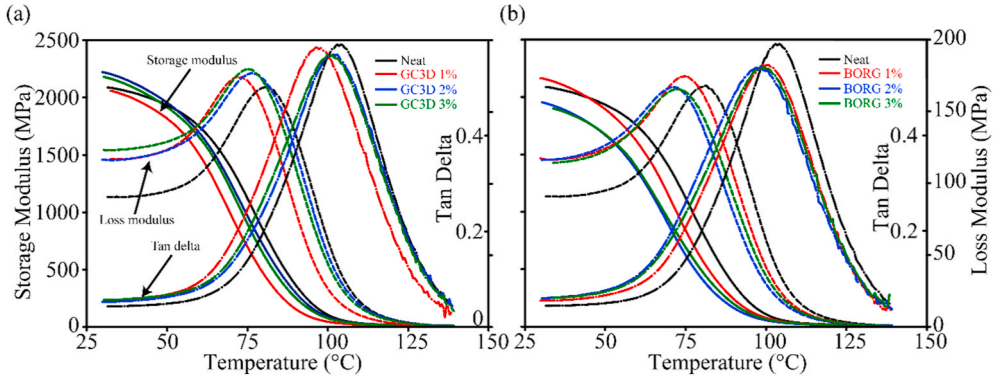

Fig. 10. DMA analysis of (a)SS/GC3D and (b) SS/BORG nanocomposites.

particles have enhanced the storage modulus of the nanocomposite systems. The filler particles localize the heat energy and prevent it from transferring to the surrounding matrix. Furthermore, the enhanced rigidity of the polymer molecules also contributes to the improvement of storage modulus by immobilizing the polymer chain molecules [11].

However, as the filler loading increases, the dispersion becomes ineffective due to the agglomeration of particles Similarly, loss modulus is also affected by the polymer-particle interaction. The dispersion of filler materials strongly restricts the mobility of surrounding matrix resulting in high dissipation of energy [80–82].

4. Conclusion

Georgian and Brazilian clays available from the natural and renewable sources were successfully modified using ultrasonication in the presence of decalin and by using quaternary ammonium salts, respectively. XRD and TEM results confirmed the particle size reduction and expanded clay structure. The results suggested that ultrasonication has effectively reduced the particle size and modified the Georgian clay. Significant improvement in flexure properties was observed for Super Sap 100/1000 epoxy nanocomposite systems with modified clay modified clay particles. However, there is no significant change in strain at maximum stress due to the ductile nature of the bio-based content present in the Super Sap 100/1000 epoxy system. Hence, these results suggest that modified nano clay particles can be successfully used as fillers for both structural engineering and biomedical applications. The topology from the fractured surfaces revealed the crack propagation paths which influenced the strength of the specimens. The neat epoxy system exhibited brittle failure whereas SS/GC3D has shown improvement in ductility with the cracks propagating around ridges and SS/BORG failed due to the presence of voids. The strength of the composites can be further improved if the voids and agglomerations are maintained carefully. The major degradation temperatures of the composites have shown noteworthy improvement from 7° to 25 °C with the infusion of modified clay particles. TMA and DMA analysis also have shown significant improvement in dimensional stability and storage moduli due to the reinforcement of 1–3 wt% modified nano clay particles. In view of this, it can be articulated that the modified nano clay particles can effectively serve as natural fillers for bio-based Super Sap 100/1000 epoxy resin system and other bio-based polymers thus developing a green material for potential applications such as coatings, adhesives, laminates, tooling and castings.

Declaration of competing interest

The authors declare that they have no known competing financial interests or personal relationships that could have appeared to influence the work reported in this paper.

Acknowledgements

The authors acknowledge the financial support of NSF-RISE #1459007, NSF-CREST#, 1735971 and NSF-MRI-1531934.

Appendix A. Supplementary data

Supplementary data to this article can be found online at https://doi.org/10.1016/j.matchemphys.2020.123821.

Credit author statement

The manuscript was written through contributions of all authors. All authors have given approval to the final version of the manuscript.

References

[1] H. Salam, Y. Dong, I. Davies, Development of Biobased Polymer/clay Nanocomposites: A Critical Review, Elsevier Ltd, 2015, https://doi.org/10.1016/B978-0-08-100079-3.00006-5.
[2] A. Azeez, K. Rhee, S. Park, D. Hui, Epoxy clay nanocomposites-processing, properties and applications: a review, Compos. B Eng. 45 (2012) 308–320, https://doi.org/10.1016/j.compositesb.2012.04.012.
[3] F.L. Jin, X. Li, S.J. Park, Synthesis and application of epoxy resins: a review, J. Ind. Eng. Chem. 29 (2015) 1–11, https://doi.org/10.1016/j.jiec.2015.03.026.
[4] A. Saikia, N. Karak, Castor oil based epoxy/clay nanocomposite for advanced applications, Am. J. Eng. Appl. Sci. 9 (2015) 31–40, https://doi.org/10.3844/ajeassp.2016.31.40.
[5] Z. Ahmadi, Epoxy in nanotechnology: a short review, Prog. Org. Coating 132 (2019) 445–448, https://doi.org/10.1016/j.porgcoat.2019.04.003.
[6] L. Wang, X. Shui, X. Zheng, J. You, Y. Li, Investigations on the morphologies and properties of epoxy/acrylic rubber/nanoclay nanocomposites for adhesive films, Compos. Sci. Technol. 93 (2014) 46–53, https://doi.org/10.1016/j.compscitech.2013.12.023.
[7] M.M. Rahman, M. Hosur, S. Zainuddin, K.C. Jajam, H.V. Tippur, S. Jeelani, Mechanical characterization of epoxy composites modified with reactive polyol diluent and randomly-oriented amino-functionalized MWCNTs, Polym. Test. 31 (2012) 1083–1093, https://doi.org/10.1016/j.polymertesting.2012.08.010.
[8] C.A. May, Epoxy Resins: Chemistry and Technology, second ed., Marcel Dekker, 1987.
[9] N. Platzer, Encyclopedia of polymer science and engineering, J. Polym. Sci. C Polym. Lett. 25 (1987) 268, https://doi.org/10.1002/pol.1987.140250612, 268.
[10] B. Ellis, Chemistry and Technology of Epoxy Resins, Springer Netherlands, Dordrecht, 1993, https://doi.org/10.1007/978-94-011-2932-9.
[11] M.S. Lakshmi, B. Narmadha, B.S.R. Reddy, Enhanced thermal stability and structural characteristics of different MMT-Clay/epoxy-nanocomposite materials, Polym. Degrad. Stabil. 93 (2008) 201–213, https://doi.org/10.1016/j.polymdegradstab.2007.10.005.
[12] S.K. Kumar, R. Krishnamoorti, Nanocomposites: structure, phase behavior, and properties, Annu. Rev. Chem. Biomol. Eng. 1 (2010) 37–58, https://doi.org/10.1146/annurev-chembioeng-073009-100856.
[13] Y. Mai, Z. Yu, Polymer Nanocomposites, Woodhead Publ., 2006.
[14] P.M. Ajayan, L.S. Schadler, P.V. Braun, Nanocomposite Science and Technology, Wiley, 2003.
[15] P. Jiang, S. Zhang, S. Bourbigot, Z. Chen, S. Duquesne, M. Casetta, Surface grafting of sepiolite with a phosphaphenanthrene derivative and its flame-retardant mechanism on PLA nanocomposites, Polym. Degrad. Stabil. 165 (2019) 68–79, https://doi.org/10.1016/j.polymdegradstab.2019.04.012.
[16] P.A. Schroeder, Kaolin, New Georg, Encycl., 2013.
[17] H.H. Murray, Traditional and new applications for kaolin, smectite, and palygorskite: a general overview, Appl. Clay Sci. 17 (2000) 207–221, https://doi.org/10.1016/S0169-1317(00)00016-8.
[18] C.C. Harvey, H.H. Murray, Industrial clays in the 21st century: a perspective of exploration, technology and utilization, Appl. Clay Sci. 11 (1997) 285–310, https://doi.org/10.1016/S0169-1317(96)00028-2.
[19] C. Gomes, Argilas: Aplicações Na Indústria, Bulhosa Livreiros, 2002.
[20] W.D. Keller, H.H. Murray, W.M. Bundy, Kaolin Genesis and Utilization, The Clay Minerals Society, West Lafayette, IN, 1993.
[21] E. Galan, P. Aparicio, I. Gonzalez, A. Miras, Contribution of multivariate analysis to the correlation of some properties of kaolin with its mineralogical and chemical composition, Clay Miner. 33 (1998) 65–75, https://doi.org/10.1180/000985598545435.
[22] L. Su, X. Zeng, H. He, Q. Tao, S. Komarneni, Preparation of functionalized kaolinite/epoxy resin nanocomposites with enhanced thermal properties, Appl. Clay Sci. 148 (2017) 103–108, https://doi.org/10.1016/j.clay.2017.08.017.
[23] M. Rajaei, N.K. Kim, S. Bickerton, D. Bhattacharyya, A comparative study on effects of natural and synthesised nano-clays on the fire and mechanical properties of epoxy composites, Compos. B Eng. 165 (2019) 65–74, https://doi.org/10.1016/j.compositesb.2018.11.089.
[24] L. Cabedo, E. Giménez, J.M. Lagaron, R. Gavara, J.J. Saura, Development of EVOH-kaolinite nanocomposites, Polymer 45 (2004) 5233–5238, https://doi.org/10.1016/j.polymer.2004.05.018.
[25] Q. Zhang, Q. Liu, J.E. Mark, I. Noda, A novel biodegradable nanocomposite based on poly (3-hydroxybutyrate-co-3-hydroxyhexanoate) and silylated kaolinite/silica core–shell nanoparticles, Appl. Clay Sci. 46 (2009) 51–56, https://doi.org/10.1016/j.clay.2009.07.008.
[26] F. Franco, L.A. Pérez-Maqueda, J.L. Pérez-Rodríguez, The effect of ultrasound on the particle size and structural disorder of a well-ordered kaolinite, J. Colloid Interface Sci. 274 (2004) 107–117, https://doi.org/10.1016/j.jcis.2003.12.003.
[27] F. Franco, L.A. Ṕrez-Maqueda, J.L. Pérez-Rodriguez, Influence of the particle-size reduction by ultrasound treatment on the dehydroxylation process of kaolinites, J. Therm. Anal. Calorim. 78 (2004) 1043–1055, https://doi.org/10.1007/s10973-005-0469-0.
[28] T.A. Hassan, V.K. Rangari, R.K. Rana, S. Jeelani, Sonochemical effect on size reduction of CaCO3 nanoparticles derived from waste eggshells, Ultrason. Sonochem. 20 (2013) 1308–1315, https://doi.org/10.1016/j.ultsonch.2013.01.016.
[29] S. Zinatloo-Ajabshir, S. Mortazavi-Derazkola, M. Salavati-Niasari, Nd2O3-SiO2 nanocomposites: a simple sonochemical preparation, characterization and photocatalytic activity, Ultrason. Sonochem. 42 (2018) 171–182, https://doi.org/10.1016/j.ultsonch.2017.11.026.
[30] K.S. Suslick, The chemistry of ultrasound, in: Encycl. Br. Yearb. Sci. Futur, Encyclopaedia Britannica, Chicago, 1994, pp. 138–155, 1994.
[31] I. Krásný, L. Lapčík, B. Lapčíková, R.W. Greenwood, K. Šafářová, N.A. Rowson, The effect of low temperature air plasma treatment on physico-chemical properties of kaolinite/polyethylene composites, Compos. B Eng. 59 (2014) 293–299, https://doi.org/10.1016/j.compositesb.2013.12.019.
[32] S.N. Das, T.K. Khastgir, D.K. Chakraborty, Effect of filler blend composition on the electrical and mechanical properties of conductive AVE composite, Proj. Euclid. 8 (2002) 457–634.
[33] Y. Li, B. Zhang, X. Pan, Preparation and characterization of PMMA–kaolinite intercalation composites, Compos. Sci. Technol. 68 (2008) 1954–1961, https://doi.org/10.1016/j.compscitech.2007.04.003.
[34] F. Franco, L.A. Pérez-Maqueda, J.L. Pérez-Rodríguez, The influence of ultrasound on the thermal behaviour of a well ordered kaolinite, Thermochim. Acta 404 (2003) 71–79, https://doi.org/10.1016/S0040-6031(03)00065-0.
[35] L. Amorim, C. Gomes, H. Lira, Bentonites from Boa Vista, Brazil: physical, mineralogical and rheological properties, Mater 7 (2004) 583–593.
[36] F. Valenzuela-Díaz, Preparation of organophilic clays from a Brazilian smectitic clay, Key Eng. Mater. 189–191 (2001) 203–207.
[37] F.R. Valenzuela-Diaz, L.D.V. de Abreu, P. de S. Santos, Hot sodium cation exchange in light-green smectitic clay from campina grande, Paraiba. Ceramica 42 (1997) 290–293.
[38] M.F. Delbem, T.S. Valera, F.R. Valenzuela-Diaz, N.R. Demarquette, Modification of a brazilian smectite clay with different quaternary ammonium salts, Quim. Nova 33 (2010) 309–315.
[39] R. Barbosa, E.M. Araújo, T.J.A. Melo, E.N. Ito, Comparison of flammability behavior of polyethylene/Brazilian clay nanocomposites and polyethylene/flame retardants, Mater. Lett. 61 (2007) 2575–2578, https://doi.org/10.1016/j.matlet.2006.09.055.
[40] E.M. Araújo, R. Barbosa, A.W.B. Rodrigues, T.J.A. Melo, E.N. Ito, Processing and characterization of polyethylene/Brazilian clay nanocomposites, Mater. Sci. Eng. (2007) 445–446, https://doi.org/10.1016/j.msea.2006.09.012, 141–147.
[41] E.M. Araújo, T.J.A. Mélo, L.N.L. Santana, G.A. Neves, H.C. Ferreira, H.L. Lira, L. H. Carvalho, M.M. A'vila, M.K.G. Pontes, I.S. Araújo, The influence of organo-bentonite clay on the processing and mechanical properties of nylon 6 and polystyrene composites, Mater. Sci. Eng. B 112 (2004) 175–178, https://doi.org/10.1016/j.mseb.2004.05.027.
[42] E.M. Araújo, R. Barbosa, C.R.S. Morais, L.E.B. Soledade, A.G. Souza, M.Q. Vieira, Effects of organoclays on the thermal processing of pe/clay nanocomposites, J. Therm. Anal. Calorim. 90 (2007) 841–848, https://doi.org/10.1007/s10973-006-7504-7.
[43] A.V. Ortiz, J.G. Teixeira, M.G. Gomes, R.R. Oliveira, F.R.V. Díaz, E.A.B. Moura, Preparation and characterization of electron-beam treated HDPE composites reinforced with rice husk ash and Brazilian clay, Appl. Surf. Sci. (2014), https://doi.org/10.1016/j.apsusc.2014.03.075.
[44] J.L. Alves, P.T.V. Rosa, V. Realinho, M. Antunes, J.I. Velasco, A.R. Morales, The effect of Brazilian organic-modified montmorillonites on the thermal stability and fire performance of organoclay-filled PLA nanocomposites, Appl. Clay Sci. 194 (2020) 105697, https://doi.org/10.1016/j.clay.2020.105697.
[45] J.L. Alves, P. de T.V. e Rosa, V. Realinho, M. Antunes, J.I. Velasco, A.R. Morales, Influence of chemical composition of Brazilian organoclays on the morphological, structural and thermal properties of PLA-organoclay nanocomposites, Appl. Clay Sci. 180 (2019) 105186, https://doi.org/10.1016/j.clay.2019.105186.
[46] Entropy Resins Inc., SUPER SAP® 100/1000 SYTEM, 2016. https://adhesives.specialchem.com/product/p-entropy-resins-super-sap-100-1000-sytem.

[47] ASTM International, ASTM D6866-11, Standard Test Methods for Determining the Biobased Content of Solid, Liquid, and Gaseous Samples Using Radiocarbon Analysis, 2011. West Conshohocken, PA.
[48] de L.A.C.S. Andrade, W.A. Freire, S.S. Araújo, L.G.F. Vieira, A.C.F.M. Costa, L. H. Carvalho, A.S. Gomes, S.M.L. Silva, Organophilization of four differents bentonitic clays with a quaternary ammonium salt, Mater. Sci. Forum 498–499 (2005) 67–72. https://doi.org/10.4028/www.scientific.net/MSF.498-499.67.
[49] L.B. de Paiva, A.R. Morales, F.R. Valenzuela Díaz, Organoclays: properties, preparation and applications, Appl. Clay Sci. 42 (2008) 8–24, https://doi.org/10.1016/j.clay.2008.02.006.
[50] ASTM Standard D790 -10: Standard Test Methods for Flexural Properties of Unreinforced and Reinforced Plastics and Electrical Insulating Materials, 2010, https://doi.org/10.1520/D0790-10.
[51] ASTM Statndard D696-08e1, Standard Test Method for Coefficient of Linear Thermal Expansion of Plastics between − 30 ° C and 30 ° C with a Vitreous Silica Dilatometer, 2008, https://doi.org/10.1520/D0696-08E01, 08.
[52] K.S. Suslick, S.-B. Choe, A.A. Cichowlaas, M.W. Grinstaff, Sonochemical synthesis of amorphous iron, Nature 353 (1991) 414–416.
[53] V.R. Babu, S. Loganathan, G. Pugazhenthi, S. Thomas, T.O. Varghese, Chapter 2 - an overview of polymer–clay nanocomposites, in: K. Jlassi, M.M. Chehimi, S.B.T.-C.-P.N. Thomas (Eds.), Clay-polymer Nanocomposites, Elsevier, 2017, pp. 29–81, https://doi.org/10.1016/B978-0-323-46153-5.00002-1.
[54] J. Zhang, E. Manias, C.A. Wilkie, Polymerically modified layered silicates: an effective route to nanocomposites, J. Nanosci. Nanotechnol. 8 (2008) 1597–1615, https://doi.org/10.1166/jnn.2008.037.
[55] M. Valášková, M. Rieder, V. Matějka, P. Čapková, A. Slíva, Exfoliation/delamination of kaolinite by low-temperature washing of kaolinite–urea intercalates, Appl. Clay Sci. 35 (2007) 108–118, https://doi.org/10.1016/j.clay.2006.07.001.
[56] D. Sun, B. Li, Y. Li, C. Yu, B. Zhang, H. Fei, Characterization of exfoliated/delamination kaolinite, Mater. Res. Bull. 46 (2011) 101–104, https://doi.org/10.1016/j.materresbull.2010.09.031.
[57] P. Yuan, D. Tan, F. Annabi-Bergaya, W. Yan, D. Liu, Z. Liu, From platy kaolinite to aluminosilicate nanoroll via one-step delamination of kaolinite: effect of the temperature of intercalation, Appl. Clay Sci. (2013) 83–84, https://doi.org/10.1016/j.clay.2013.08.027, 68–76.
[58] K. Jlassi, I. Krupa, M.M. Chehimi, Chapter 1 - overview: clay preparation, properties, modification, in: K. Jlassi, M.M. Chehimi, S.B.T.-C.-P.N. Thomas (Eds.), Clay-polymer Nanocomposites, Elsevier, 2017, pp. 1–28, https://doi.org/10.1016/B978-0-323-46153-5.00001-X.
[59] T. Seyidoglu, U. Yilmazer, Modification and characterization of bentonite with quaternary ammonium and phosphonium salts and its use in polypropylene nanocomposites, J. Thermoplast. Compos. Mater. 28 (2015) 86–110, https://doi.org/10.1177/0892705713486123.
[60] M. Slaný, Ľ. Jankovič, J. Madejová, Structural characterization of organo-montmorillonites prepared from a series of primary alkylamines salts: mid-IR and near-IR study, Appl. Clay Sci. 176 (2019) 11–20, https://doi.org/10.1016/j.clay.2019.04.016.
[61] T. Seyidoglu, U. Yilmazer, Production of modified clays and their use in polypropylene-based nanocomposites, J. Appl. Polym. Sci. 127 (2013) 1257–1267, https://doi.org/10.1002/app.37757.
[62] J. Ma, Z. Qi, Y. Hu, Synthesis and characterization of polypropylene/clay nanocomposites, J. Appl. Polym. Sci. 82 (2001) 3611–3617, https://doi.org/10.1002/app.2223.
[63] A. Prakash, G. Sarkhel, K. Kumar, Strength optimization for kaolin reinforced epoxy composite using taguchi method, Mater. Today Proc. 2 (2015) 2380–2388, https://doi.org/10.1016/j.matpr.2015.07.175.
[64] Y. Zhou, F. Pervin, V.K. Rangari, S. Jeelani, Influence of montmorillonite clay on the thermal and mechanical properties of conventional carbon fiber reinforced composites, J. Mater. Process. Technol. 191 (2007) 347–351, https://doi.org/10.1016/j.jmatprotec.2007.03.059.
[65] R.P. Singh, M. Khait, S.C. Zunjarrao, C.S. Korach, G. Pandey, Environmental degradation and durability of epoxy-clay nanocomposites, J. Nanomater. 2010 (2010), https://doi.org/10.1155/2010/352746.
[66] B.J. Tiimob, V.K. Rangari, S. Jeelani, Effect of reinforcement of sustainable β-CaSiO3 nanoparticles in bio-based epoxy resin system, J. Appl. Polym. Sci. 131 (2014) 1–10, https://doi.org/10.1002/app.40867.
[67] F. Asuke, V.S. Aigbodion, M. Abdulwahab, O.S.I. Fayomi, A.P.I. Popoola, C. I. Nwoyi, B. Garba, Effects of bone particle on the properties and microstructure of polypropylene/bone ash particulate composites, Results Phys 2 (2012) 135–141, https://doi.org/10.1016/j.rinp.2012.09.001.
[68] H.S. Jaggi, Y. Kumar, B.K. Satapathy, A.R. Ray, A. Patnaik, Analytical interpretations of structural and mechanical response of high density polyethylene/hydroxyapatite bio-composites, Mater. Des. 36 (2012) 757–766, https://doi.org/10.1016/j.matdes.2011.12.004.
[69] M. Bashar, P. Mertiny, U. Sundararaj, Effect of nanocomposite structures on fracture behavior of epoxy-clay nanocomposites prepared by different dispersion methods, J. Nanomater. 2014 (2014), https://doi.org/10.1155/2014/312813.
[70] H. Salam, Y. Dong, I.J. Davies, A. Pramanik, The effects of material formulation and manufacturing process on mechanical and thermal properties of epoxy/clay nanocomposites, Int. J. Adv. Manuf. Technol. 87 (2016) 1999–2012, https://doi.org/10.1007/s00170-016-8572-x.
[71] B.J. Tiimob, S. Jeelani, V.K. Rangari, Eggshell reinforced biocomposite - an advanced "green" alternative structural material, J. Appl. Polym. Sci. 133 (2016) 1–10, https://doi.org/10.1002/app.43124.
[72] A. Asif, V.L. Rao, V. Saseendran, K.N. Ninan, Thermoplastic toughened layered silicate epoxy ternary nanocomposites—preparation, morphology, and thermomechanical properties, Polym. Eng. Sci. 49 (2009) 756–767, https://doi.org/10.1002/pen.21226.
[73] P.-Y. Kuo, M. Sain, N. Yan, Synthesis and characterization of an extractive-based bio-epoxy resin from beetle infested Pinus contorta bark, Green Chem. 16 (2014) 3483–3493, https://doi.org/10.1039/C2GC36073J.
[74] Y. Lu, R.C. Larock, Bio-based nanocomposites from corn oil and functionalized organoclay prepared by cationic polymerization, Macromol. Mater. Eng. 292 (2007) 863–872, https://doi.org/10.1002/mame.200700064.
[75] L.B. Fitaroni, J.A. De Lima, S.A. Cruz, W.R. Waldman, Thermal stability of polypropylene-montmorillonite clay nanocomposites: limitation of the thermogravimetric analysis, Polym. Degrad. Stabil. 111 (2015) 102–108, https://doi.org/10.1016/j.polymdegradstab.2014.10.016.
[76] K. Zhang, L. Wang, F. Wang, G. Wang, Z. Li, Preparation and characterization of modified-clay-reinforced and toughened epoxy-resin nanocomposites, J. Appl. Polym. Sci. 91 (2004) 2649–2652, https://doi.org/10.1002/app.13445.
[77] T. Liu, W.C. Tjiu, Y. Tong, C. He, S.S. Goh, T.S. Chung, Morphology and fracture behavior of intercalated epoxy/clay nanocomposites, J. Appl. Polym. Sci. 94 (2004) 1236–1244, https://doi.org/10.1002/app.21033.
[78] G.J. Withers, Y. Yu, V.N. Khabashesku, L. Cercone, V.G. Hadjiev, J.M. Souza, D. C. Davis, Improved mechanical properties of an epoxy glass-fiber composite reinforced with surface organomodified nanoclays, Compos. B Eng. 72 (2015) 175–182, https://doi.org/10.1016/j.compositesb.2014.12.008.
[79] I. Glavchev, K. Petrova, M. Ivanova, Determination of the coefficient of thermal expansion of epoxy composites, Polym. Test. 21 (2002) 177–179, https://doi.org/10.1016/S0142-9418(01)00066-6.
[80] X. Liu, Q. Wu, L.A. Berglund, H. Lindberg, J. Fan, Z. Qi, Polyamide 6/clay nanocomposites using a cointercalation organophilic clay via melt compounding, J. Appl. Polym. Sci. 88 (2003) 953–958, https://doi.org/10.1002/app.12031.
[81] F. Lionetto, A. Maffezzoli, Rheological characterization of concentrated nanoclay dispersions in an organic solvent, Appl. Rheol. 19 (2009).
[82] M.M. Rahman, S. Zainuddin, M.V. Hosur, C.J. Robertson, A. Kumar, J. Trovillion, S. Jeelani, Effect of NH2-MWCNTs on crosslink density of epoxy matrix and ILSS properties of e-glass/epoxy composites, Compos. Struct. 95 (2013) 213–221, https://doi.org/10.1016/j.compstruct.2012.07.019.